# Femtosecond laser micromachining in transparent materials

Femtosecond laser micromachining can be used either to remove materials or to change a material's properties, and can be applied to both absorptive and transparent substances. Over the past decade, this technique has been used in a broad range of applications, from waveguide fabrication to cell ablation. This review describes the physical mechanisms and the main experimental parameters involved in the femtosecond laser micromachining of transparent materials, and important emerging applications of the technology.

RAFAEL R. GATTASS AND ERIC MAZUR

**Department of Physics and School of Engineering and Applied Sciences, Harvard University, 9 Oxford Street, Cambridge, Massachusetts 02138, USA**
**e-mail: mazur@seas.harvard.edu**

Femtosecond laser micromachining was first demonstrated in 1994, when a femtosecond laser was used to ablate micrometre-sized features on silica and silver surfaces[1,2]. In less than ten years the resolution of surface ablation has improved to enable nanometre-scale precision[3,4]. Several review articles are available on femtosecond lasers[5,6], nonlinear processes[7–9], optical breakdown[7,9], surface micromachining[10,11] and the history of femtosecond laser micromachining[12]. In this review we shall focus on the femtosecond micromachining of bulk transparent materials — that is, materials that do not have any linear absorption at the wavelength of the femtosecond laser — for the fabrication of photonic devices, as well as other applications.

There are unique advantages in favour of femtosecond laser micromachining of transparent materials over other photonic-device fabrication techniques. First, the nonlinear nature of the absorption confines any induced changes to the focal volume. This spatial confinement, combined with laser-beam scanning or sample translation, makes it possible to micromachine geometrically complex structures in three dimensions. Second, the absorption process is independent of the material, enabling optical devices to be fabricated in compound substrates of different materials. Third, femtosecond laser micromachining can be used for the fabrication of an 'optical motherboard', where all interconnects are fabricated separately, before (or even after) bonding several photonic devices to a single transparent substrate.

## PHYSICAL MECHANISMS FOR FEMTOSECOND LASER MICROMACHINING

Femtosecond laser micromachining results from laser-induced optical breakdown (Box 1), a process by which optical energy is transferred to the material, ionizing a large number of electrons that, in turn, transfer energy to the lattice. As a result of the irradiation, the material can undergo a phase or structural modification, leaving behind a localized permanent change in the refractive index or even a void.

The absorption of light in a transparent material must be nonlinear because there are no allowed electronic transitions at the energy of the incident photon[7,13]. For such nonlinear absorption to occur, the electric-field strength in the laser pulse must be approximately equal to the electric field that binds the valence electrons in the atoms — of the order of $10^9$ V m$^{-1}$, corresponding to a laser intensity of $5 \times 10^{20}$ W m$^{-2}$ (ref. 9). To achieve such electric-field strengths with a laser pulse, high intensities and tight focusing are required. For example, a 1-μJ, 100-fs laser pulse must be focused to a 200-μm$^2$ area. The tight focusing and the nonlinear nature of the absorption make it possible to confine the absorption to the focal volume inside the bulk of the material without causing absorption at the surface, yielding micromachined volumes as small as 0.008 μm$^3$ (ref. 14).

During irradiation, the laser pulse transfers energy to the electrons through nonlinear ionization[15,16]. For pulse durations greater than 10 fs, the nonlinearly excited electrons are further excited through phonon-mediated linear absorption, until they acquire enough kinetic energy to excite other bound electrons — a process called avalanche ionization. When the density of excited electrons reaches about $10^{29}$ m$^{-3}$, the electrons behave as a plasma with a natural frequency that is resonant with the laser — leading to reflection and absorption of the remaining pulse energy[15,17].

Figure 1 shows the timescales for a number of relevant physical processes involved in femtosecond laser micromachining. Part of the optical energy absorbed by the electrons is transferred to the lattice over a picosecond timescale. Within a couple of nanoseconds, a pressure or a shock wave separates from the dense, hot focal volume[18,19,20]. On the microsecond timescale, the thermal energy diffuses out of the focal volume. At a sufficiently high energy these processes cause melting or non-thermal ionic motion and leave behind permanent structural changes[21].

Understanding the different timescales involved in converting the laser pulse energy into a structural change provides an insight into why ultrashort laser pulses are well suited for micromachining applications. Laser-induced damage has been studied since the early days of the laser[12], but damage caused by femtosecond laser pulses is fundamentally different from damage caused by laser pulses with a duration greater than one picosecond. For pulses of subpicosecond duration, the timescale over which the electrons are excited is smaller than the electron–phonon scattering time (about 1 ps). Thus, a femtosecond laser pulse ends before the electrons thermally

excite any ions. Heat diffusion outside the focal area is minimized, increasing the precision of the method[22,23]. Additionally, femtosecond laser processing is a deterministic process because no defect electrons are needed to seed the absorption process; enough seed electrons are generated through nonlinear ionization from the first tens of femtoseconds of the pulse[1,16]. The confinement and repeatability of the nonlinear excitation make it possible to use the femtosecond-laser-induced damage for practical purposes.

## BULK DAMAGE AND EXPERIMENTAL PARAMETERS

If the energy transfer from the laser pulse was caused solely by nonlinear ionization, the intensity required to induce a permanent change would depend nonlinearly on the bandgap of the irradiated material. The probability of light being absorbed in a material that has a bandgap energy equivalent to $N$ photons through nonlinear absorption is $I^N$, where $I$ is the electric-field intensity. Because the bandgap energy (and therefore $N$) varies from material to material, the nonlinear absorption would vary enormously. Experimentally, however, the threshold intensity, $I_{th}$, required to damage a material is found to vary only very slightly with the bandgap energy (Fig. 2), indicating the importance of avalanche ionization, which depends linearly on $I$. Because of this low dependence on the bandgap energy, femtosecond laser micromachining can be used in a broad range of materials.

The intensity required to damage a material is determined by three experimental parameters: the laser pulse duration, $\tau$, the pulse energy, $E$, and the focusing numerical aperture, NA. The minimum $\tau$ and maximum $E$ are usually fixed by the laser system, leaving only the variable NA free. At first glance, the effects of $\tau$, $E$ and NA on the intensity at a given wavelength, $\lambda$, would be expected to follow[24]:

$$I \propto E\,\mathrm{NA}^2/[\tau\lambda^2(1-\mathrm{NA}^2)]. \qquad (1)$$

However, as shown below, the dependence of $I_{th}$ for micromachining on these three parameters does not follow the expected behaviour.

The dependence of $I_{th}$ on $\tau$ has been explored for values of $\tau$ down to 10 fs, and experiments do not reveal the expected inverse relation between $I$ and $\tau$ given by equation 1. For $\tau > 10$ ps, $I_{th}$ varies as $\tau^{1/2}$, indicating that Joule heating of the electrons excited at the beginning of the pulse is responsible for the optical damage[17]. For $\tau < 10$ ps, $I_{th}$ increases threefold for a tenfold increase in $\tau$ (ref. 25). The low level of dependence on $\tau$ is due to avalanche ionization: nonlinear ionization creates the initial seed population, but the linear dependence of the avalanche process on $I$ is responsible for the high excitation density necessary for micromachining[13,16]. The relatively small effect of altering $\tau$ on $I_{th}$ provides flexibility in the choice of laser system, which is important for commercial applications of femtosecond laser micromachining.

For conditions where $\tau$ and NA are fixed, the absorption process has a strong dependence on $E$. The minimum $E$ required for the nonlinear absorption that seeds electrons is the threshold energy. When $E$ is kept close to this threshold, the absorption produces a change in the index of refraction that is localized to the focal volume. The magnitude of the refractive-index change varies from material to material, with both positive and negative index contrasts being reported. The refractive-index change is usually of the same order of magnitude as that found in standard optical fibres, that is, around $10^{-3}$ (refs 26–30). The change in the refractive index is not spatially homogeneous, and the mechanisms responsible for the spatially dependent change are under investigation; stress-induced changes, densification, changes in effective fictive temperature, and colour-centre formation contribute differently for each material system and for each set of processing conditions[27,30–35]. Increasing $E$ beyond the threshold increases the size of the affected area and the average energy of the plasma. As the plasma energy increases, ionic shielding is reduced causing Coulomb repulsion between ions. A surge of Coulomb repulsion with sufficient energy leads to void formation[32]. Even if $E$ is not large enough for void formation, interference between the incident pulse and the electron plasma can occur, resulting in a

## Box 1 A nonlinear absorption process

When a femtosecond laser pulse with a high enough pulse peak intensity is focused into a material, optical breakdown is observed (Fig. B1a). The laser pulse energy is partially transferred to the electrons in the short duration of the pulse. The highly excited electrons thermalize with the ions and alter the material permanently. Depending on the degree of excitation, cracking, void formation or localized melting occurs. In the absence of impurities, carriers are generated initially by multiphoton absorption, promoting electrons from the valence to the conduction band (Fig. B1b). Several photons must be incident on an electron at the same time for the process to occur with a high probability. For example, the six-photon absorption cross-section of fused silica is approximately $6 \times 10^4$ m$^{-3}$ ps$^{-1}$ (m$^2$/TW)$^6$ (ref. 13). The micromachined feature size will depend on many experimental parameters: $E$ (the pulse energy), $\tau$ (the pulse duration) and NA (the focusing numerical aperture). However, under special conditions, exposure to multiple pulses can further change the feature size. Figure B1c shows microscope images of the large variation in the features of femtosecond-laser-induced changes, due to experimental conditions.

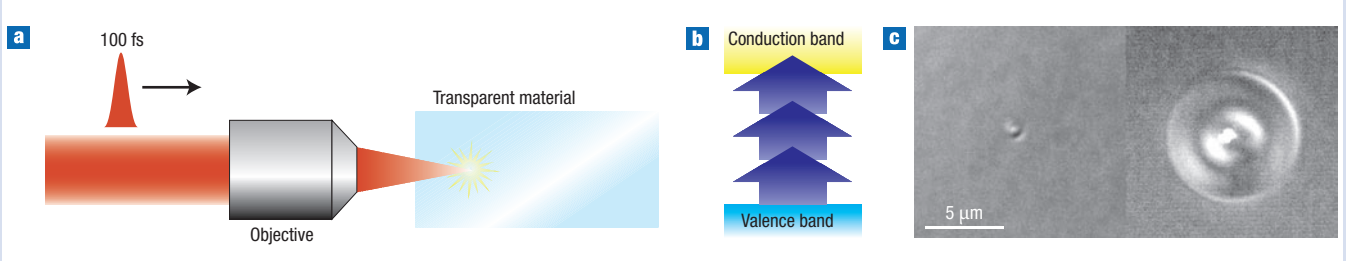


**Figure B1** Femtosecond laser micromaching process. **a**, Schematic of the laser incident on a transparent material. **b**, Diagram of the excitation of electrons to the conduction band. **c**, Microscope images showing the large variation in the feature characteristics depending on the experimental conditions. Left: single 10-nJ pulse and right: 25,000 5-nJ pulses at a frequency of 25 MHz (both with the same focal spot).

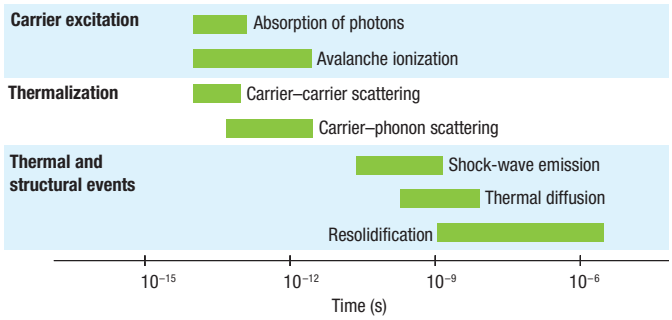


**Figure 1** Timescale of the physical phenomena associated with the interaction of a femtosecond laser pulse with transparent materials. The green bars represent typical timescales for the relevant process. Note that although the absorption of light occurs at the femtosecond timescale, the material can continue to undergo changes microseconds later.

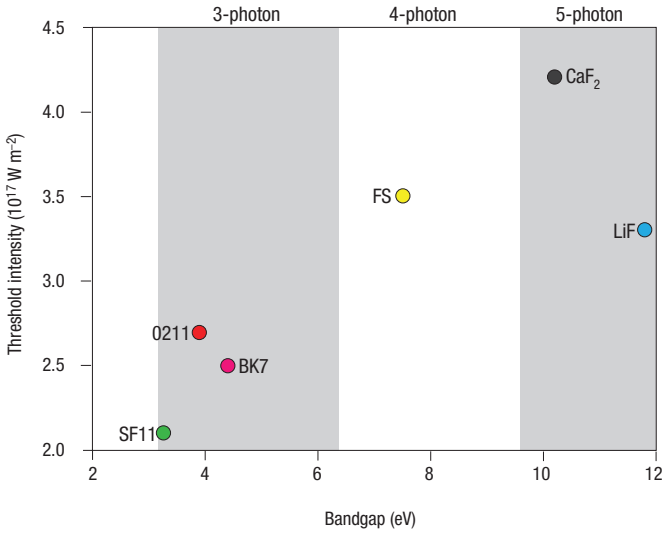


**Figure 2** Bandgap dependence of the threshold fluence for femtosecond laser micromachining by pulses centred at a wavelength of 800 nm with a duration of 100 fs. The bandgaps of the materials depicted by coloured circles range over various multiphoton orders for the incident photon energy of 1.55 eV. The threshold intensity does not follow a power law, increasing by only about a factor of two as the energy required to span the bandgap increases from three to five photons. Because femtosecond laser micromachining is nearly independent of the bandgap of the material it can be used in a wide range of materials.

birefringent periodic modulation[36–40]. Most photonic applications use values of $E$ that are close to the absorption threshold and thus result in changes in the refractive index.

The third experimental parameter, NA, determines the width of the focal volume and therefore the resulting feature size. The range of NAs that can be used, however, is limited. Numerical apertures larger than 0.002 are required to achieve $I_{th}$ with the millijoule values of $E$ that are available with commercial amplified laser systems. In practice, the minimum NA is significantly larger than this value because at low NA, two nonlinear processes compete with the energy deposition: self-focusing and white-light generation. Self-focusing — an intensity-dependent distortion of the propagating wavefront — manifests itself when the laser-pulse power exceeds a critical value (about 4 MW for fused silica)[41], causing the pulse to collapse into a filament with a diameter that is smaller than the one expected from the external focusing[42,43]. White-light generation causes spectral broadening of the laser pulse as it propagates[44]. For NAs below 0.1, the intensity threshold of both these nonlinear processes is lower than $I_{th}$ (refs 24,45). The nonlinear effects reduce the repeatability and the control over the micromachining processes, and the resulting feature size is no longer determined by the external focusing[24,46,47].

At NAs close to or larger than unity, femtosecond laser micromachining can be accomplished in glasses with femtosecond laser oscillators delivering just nanojoules of energy per pulse[48]. Laser oscillators, with their high repetition rates, can be used to increase the area that can be patterned in a given amount of time and to allow control over the size of the micromachined area. In oscillator-only machining, the time interval between pulses is smaller than the heat diffusion time (about 1 μs). The energy delivered by each pulse accumulates at the focus before diffusing out, forming a point source of heat[48,49]. Because of this ensuing diffusion, the feature sizes can significantly exceed the focal volume, creating spherical features up to 50 μm in diameter, using a focal spot of only 0.5 μm (ref. 48). Although at high NAs, the NA sets the threshold energy, the feature size is controlled by the number of incident pulses.

Besides altering $I$, the NA also affects the geometry of the final structure in single-shot experiments. Above an NA of 0.6, the micromachined features are almost spherically symmetric; below this value, the resulting structures become larger and asymmetric. Changing the spatial profile and divergence of the input beam prior to focusing, such that the focal-spot profile is closer to a symmetric circular cross-section, can mitigate the asymmetry[50,51]. Beam shaping to alter the final geometry at low NAs remains an active topic of research.

## PHOTONIC APPLICATIONS

Femtosecond micromachining has been used to fabricate photonic devices using a variety of transparent substrates, including glasses, crystals and polymers. Owing to their high purity and large transparency window, glasses and crystals are commonly used as base materials. A wide variety of femtosecond-laser-micromachined devices, discussed in more detail below, have been demonstrated using glasses and crystals, including waveguides, active devices, filters and resonators.

The use of transparent polymers as a substrate material for fabrication presents advantages over other transparent materials. First, for polymer processing, $I_{th}$ is at least one order of magnitude lower than for glass processing. Polymers are also an attractive medium owing to the ease with which dopants can be incorporated into them, the diversity of available compositions and physical properties, and their low cost. However, compared with glasses and crystals, polymers have higher transmission losses. So far only a few photonic devices have been directly fabricated in polymers, such as ring-mode[52] and single-mode[53] waveguides in polymethylmethacrylate.

### WAVEGUIDES

Along with data storage[14], waveguide fabrication was one of the first demonstrations of the potential of femtosecond laser micromachining for photonic applications[30,54]. Femtosecond-laser-micromachined waveguides can serve as interconnects in a variety of host glasses, and have opened up the possibility of three-dimensional layering of waveguides. The pulse energy required for fabricating devices can be as low as a few nanojoules, requiring only a laser oscillator[26,48] (see, for example, Fig. 3a). The

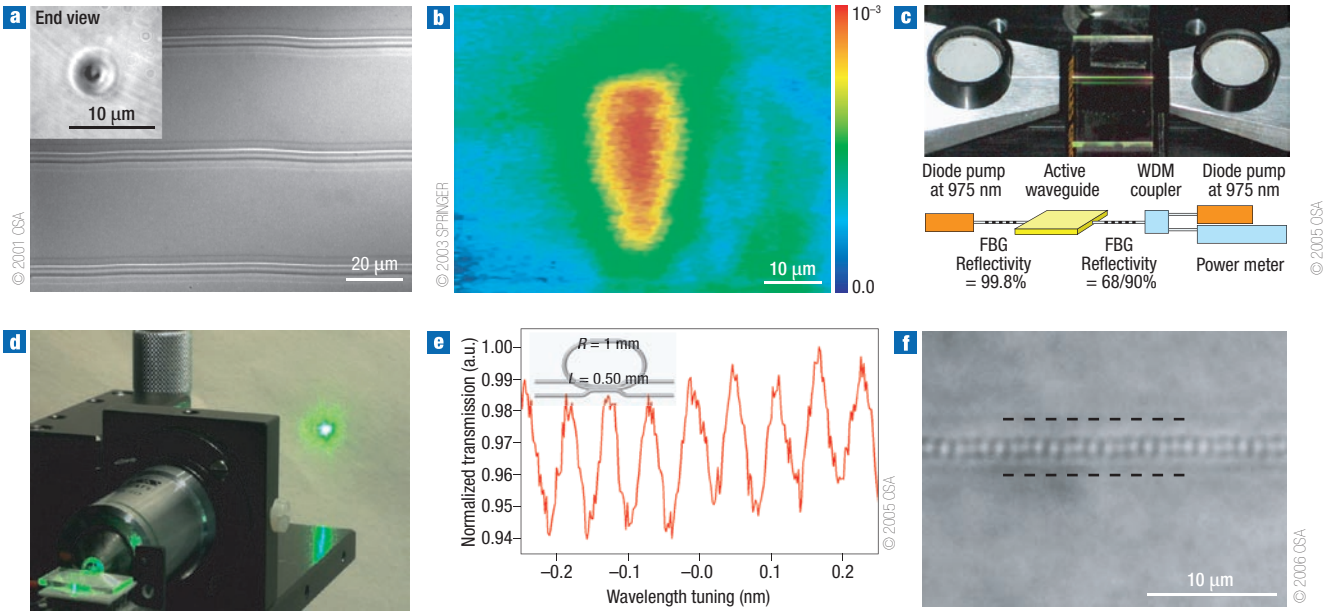


**Figure 3** Photonic applications of femtosecond laser micromachining. **a**, Optical microscope image of an oscillator-only femtosecond-laser-micromachined waveguide inside bulk glass. The inset shows one end face of the waveguide. Reprinted with permission from ref. 48. **b**, Measured refractive-index profile of a waveguide micromachined using a 0.45-NA objective with the laser beam incident from the top. False colour bar added to show the magnitude of the refractive-index change. Reproduced with permission from ref. 60. **c**, Image of a femtosecond laser micromachined lasing waveguide. FBG is fibre Bragg grating and WDM is wavelength-division multiplexer. Courtesy of Roberto Osellame. **d**, Image of a frequency conversion waveguide in a lithium niobate crystal. Courtesy of Stefan Nolte. **e**, Normalized transmission through the resonator versus wavelength (relative to the laser centre wavelength of 800 nm). The inset shows a schematic of a vertical resonator design. $R$ is the radius of curvature and $L$ is the overlap length. Reprinted with permission from ref. 71. **f**, Optical micrograph of a waveguide Bragg grating structure. The horizontal black lines indicate the edge of the waveguide. Reprinted with permission from ref. 72.

oscillator-only technique increases the rate of fabrication by three to four orders of magnitude, and also enables simple control over the cross-sectional diameter without altering the focusing conditions. Although femtosecond laser fabrication is a serial process, 10-μm waveguides spaced by 10 μm can be micromachined over an area of $10 \times 10$ mm$^2$ in about 10 minutes. Because there is no need for either a mask or post-development processing, the rate of fabrication using femtosecond lasers is now approaching that of lithographic techniques.

Over the past decade, the transmission losses, refractive-index contrast and bending radii of femtosecond-laser-micromachined interconnects have been characterized. Transmission losses are of the order of 0.1 dB mm$^{-1}$ for a large variety of materials and processing conditions[27–29,49,55–58]. The spatial profile of the refractive index of waveguides is strongly dependent on the material and the processing conditions[26–30,59], and is close to that of a fibre for fused silica substrates[27,60] (see, for example, Fig. 3b). Additionally, minimum bending radii of the order of tens of millimetres have been achieved[55,58]. Photonic-circuit designs might require micromachining interconnects across several substrates. Optically connected waveguides have already been fabricated in bonded doped and undoped phosphate glass[60], and also through multiple pieces of glass separated by air gaps[61].

## ACTIVE DEVICES

The initial application of femtosecond laser micromachining to active devices involved devices with optical gain[62]. Both femtosecond-laser-micromachined amplifiers[62,63] with a gain of 0.25 dB mm$^{-1}$ (ref. 64) and an Er:Yb-doped phosphate glass laser based on a femtosecond-laser-written waveguide have been demonstrated[65] (Fig. 3c). The materials used for micromachining photonic devices have not been restricted to glasses. Waveguides have been fabricated in electro–optic crystals, such as lithium niobate (albeit with no demonstration of electro–optic switching)[66]. Nonlinear frequency conversion in femtosecond-laser-micromachined waveguides in lithium niobate shows a 49% conversion efficiency over a length of 9.3 mm (see ref. 67 and Fig. 3d). The feasibility of magnetic switching has also been demonstrated with waveguide micromachining in a Faraday material, with the micromachined region showing almost no change in the Verdet constant from the non-irradiated material[68].

## FILTERS AND RESONATORS

In principle, devices fabricated with planar lithographic techniques can be fabricated with femtosecond laser micromachining. Indeed, couplers, filters and interleavers have already been demonstrated[26,28,46,55,60,69,70]. The three-dimensional degree of freedom permits the fabrication of vertical resonators, and vertical and lateral splitters[55,60,71] (see, for example, Fig. 3e). Femtosecond laser micromachining of fibre Bragg grating filters in the bulk of a material was first demonstrated using multiple exposures (Fig. 3f, ref. 72), but recently greater than 30-dB-strength Bragg gratings have been fabricated with a single exposure[73,74]. The long-term stability of the laser-induced index change makes femtosecond laser micromachining also attractive for both long-period fibre gratings[75,76] and normal gratings[77–79].

## POLYMERIZATION

The intrinsic nonlinear spatial confinement of femtosecond laser microfabrication can be used not only to process cured polymers,

but also to induce polymerization in a resin[80]. Usually referred to as two-photon polymerization[81], or laser direct writing[82], this polymerization technique makes it possible to fabricate polymer structures with a high degree of complexity. Many interesting optical applications of two-photon polymerization exist[83], most notably three-dimensional photonic crystals[84,85]. Two-photon polymerization is a large field with applications far exceeding the domain of photonics, most of which have already been reviewed[80,83].

## NEW AVENUES OF RESEARCH

### NANOSURGERY

Lasers have been used for selective targeting of structures and cells for more than four decades[86]. Until recently, this work involved pulses with durations in the range of picoseconds or longer[87]. As a consequence of these long pulse durations, large amounts of energy are required to induce a material change. Although subwavelength resolution has been reported[88], heating and shock-wave propagation leads to collateral damage[89]. In biological applications, control over the energy deposition is crucial; for cells even a minor rise in temperature leads to cell death[89]. Femtosecond laser pulses make precise energy delivery possible, resulting in clear, highly localized cuts in biological samples[90]. The ability to selectively ablate an area using femtosecond laser pulses was first demonstrated in the process of chromosome division[90], and later extended to subcellular organelles[91–93] (for example, Fig. 4a). With these initial demonstrations, femtosecond lasers have established themselves as versatile tools in biology with a broad range of applications, including selective neurosurgery for behaviour assays of the neuronal network in the roundworm, *C. elegans* (refs 94,95).

### MATERIAL PROCESSING

The controlled delivery of thermal energy during femtosecond laser micromachining can be used for material processing. Bonding of dissimilar materials is an engineering challenge because the mismatch between thermal expansion coefficients causes thermo–mechanical stress at the joint, weakening the bond[96]. Also, bonding two transparent materials requires an additional, partially opaque intermediate layer[96]. Femtosecond laser processing based on nonlinear absorption overcomes the need for this intermediate layer, and the rapid cooling strengthens the bond. For example, processing with femtosecond laser pulses forms a 14.9-MPa bond between borosilicate glasses[97,98] (Fig. 4b), a 15.3-MPa bond between transparent materials with dissimilar thermal expansion coefficients (such as borosilicate and fused silica)[96] and a 3.7-MPa bond between non-alkali glass and silicon crystal[99].

Femtosecond lasers can also be used to induce spatially selective phase transitions within a material. For example, crystals can be grown inside a piece of glass by exposing it to a series of femtosecond pulses[100,101]. The laser pulses heat the glass in the focal volume beyond the melting point, acting as a localized source of heat. Once a seed crystal is formed, the repeated heating and cooling causes these seed crystals to grow. This technique for inducing phase transitions can also be used for data-storage applications. For example, when samarium ions embedded in a glass host are irradiated with a femtosecond laser pulse, a transition from $Sm^{3+}$ to $Sm^{2+}$ is induced[102]. The exposed ions fluoresce at a different wavelength from the unexposed ions, and so each exposed area can act as a data-storage bit (Fig. 4c).

### MICROFLUIDIC DEVICES

The fast automated and parallel processing of small quantities of fluid requires an increasing miniaturization of chemical and biological set-ups[103–105]. So far the fabrication of such so-called microfluidic devices is mainly planar. Because the dimensions required for channels, valves and other components are within the realm of femtosecond-laser-micromachining capabilities, three-dimensional microfluidic devices have become feasible. Three-dimensional channel fabrication was demonstrated by hydrofluoric acid (HF) etching of regions in silica that had been exposed to femtosecond laser pulses (for example, Fig. 5a). Although HF etches silica too, the laser-exposed material reacts more readily with HF than unexposed areas[106]. Alternatively, the etching rate can be increased by selective precipitation of a crystalline phase inside photosensitive glasses that have been irradiated with femtosecond laser pulses, enabling the fabrication of channels[107] and complete so-called 'micro total analysis' systems[108]. Although the laser processing time for a micro-total-analysis system is large compared with the time required for lithographic and replication processing, femtosecond laser micromachining allows new channel geometries and glass-based devices. Femtosecond laser micromachining also opens the possibility for direct integration with optical detection by *in situ* fabrication of waveguides[109].

### RAPID PROTOTYPING

Because femtosecond laser micromachining does not require any mask or post-development steps, it is a suitable technique for rapid

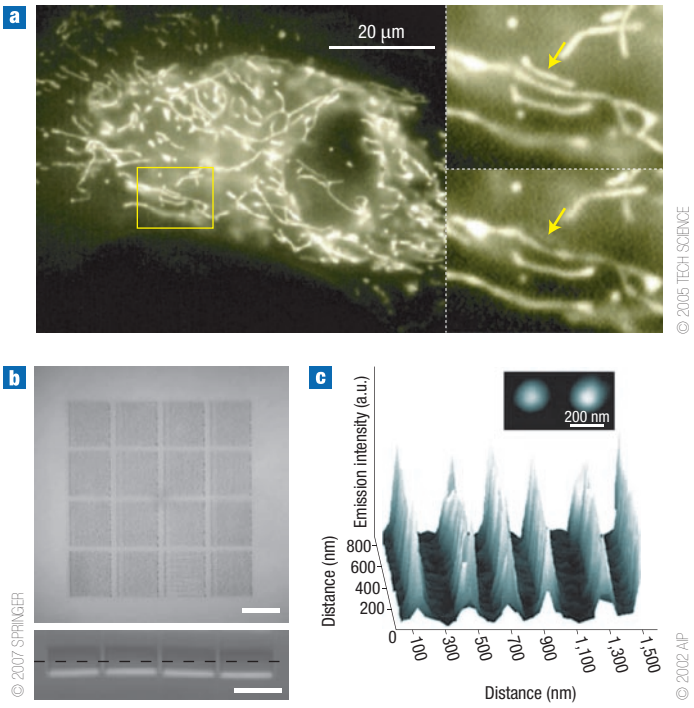


**Figure 4** Example applications of femtosecond micromachining in biology, material processing and data storage. **a**, Ablation of a single mitochondrion in a living cell. Fluorescence microscopic image showing multiple mitochondria in yellow before femtosecond laser irradiation. Target mitochondrion (marked by arrow) before (top inset) and after (bottom inset) laser ablation with 2-nJ, 100-fs pulses. Reprinted with permission from ref. 92. **b**, Microscope optical image of a femtosecond laser bonded borosilicate glass interface. Top view (top) and side view (bottom) of the joining area bonded using 1-μJ pulse energy and 0.1-mm $s^{-1}$ translation velocity. The scale bar is 100 μm. Reprinted with permission from ref. 98. **c**, Photoluminescence emission of femtosecond photoreduced $Sm^{2+}$ ions. The inset shows a samarium-ion bit that has 200-nm resolution. Reprinted with permission from ref. 102.

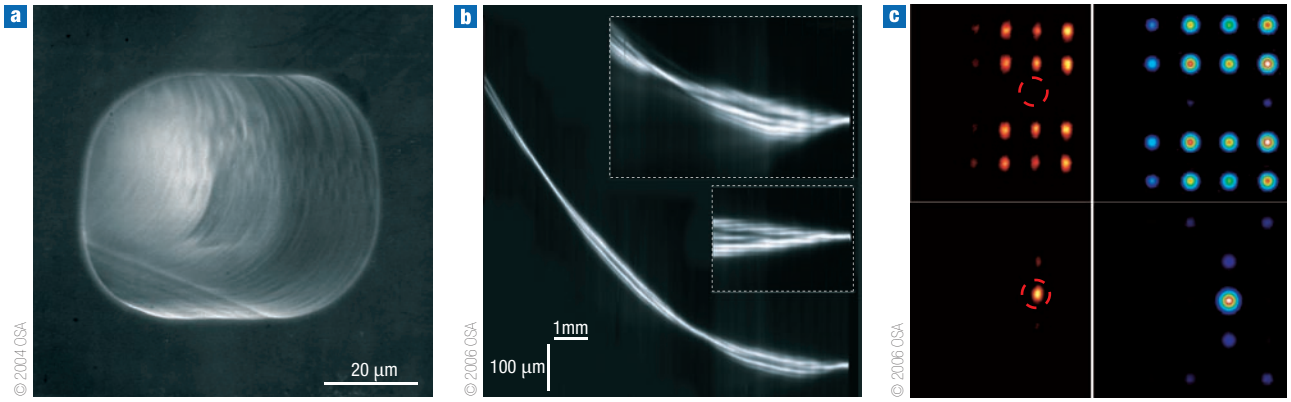


**Figure 5** Examples of microfluidic and rapid prototyping applications of femtosecond micromachining. **a**, Scanning electron micrograph of a microfluidic channel fabricated by HF-etching femtosecond-micromachined areas inside fused silica. Reprinted with permission from ref. 113. **b**, Fluorescence imaging of Bloch oscillations inside a bulk piece of glass for the central waveguide excitation of a straight array with period $a = 10$ μm. The top inset shows a curved array with radius of curvature $R = 77$ mm and period $a = 10$ μm. The bottom inset shows a curved array with $R = 77$ mm and $a = 8$ μm. Reprinted with permission from ref. 110. **c**, Measured (right) and theoretical (left) outputs from a square waveguide array at a peak power of 40 kW (top) and 1,000 kW (bottom). Reprinted with permission from ref. 111.

prototyping of photonic devices. Arrays of curved waveguides were micromachined in a glass substrate doped with a fluorescent molecule, to study the optical equivalent of Bloch oscillations (Fig. 5b, ref. 110). Two-dimensional arrays of waveguides were used to study spatial solitons[111]. Figure 5c shows the transition between a delocalized state and a spatial soliton as the pulse intensity through these coupled waveguides is increased. In both studies, the short turnaround time of femtosecond laser micromachining has been used to optimize the fabricated structures and demonstrate new aspects of waveguide coupled-mode theory[112].

## CONCLUSION

Femtosecond laser micromachining presents unique capabilities for three-dimensional, material-independent, subwavelength processing. It enables the fabrication of three-dimensional photonic devices with far greater ease than lithography, and the field is maturing at an extraordinary pace. Because femtosecond laser micromachining also holds great promise beyond the field of photonics, it is a technology that creates new markets for the laser industry and enables innovative applications.

doi:10.1038/nphoton.2008.48

## References


1. Du, D., Liu, X., Korn, G., Squier, J. & Mourou, G. Laser-induced breakdown by impact ionization in $SiO_2$ with pulse widths from 7 ns to 150 fs. *Appl. Phys. Lett.* **64,** 3071–3073 (1994).
2. Pronko, P. P. *et al.* Machining of submicron holes using a femtosecond laser at 800-nm. *Opt. Commun.* **114,** 106–110 (1995).
3. Joglekar, A. P. *et al.* A study of the deterministic character of optical damage by femtosecond laser pulses and applications to nanomachining. *Appl. Phys. B* **77,** 25–30 (2003).
4. Chimmalgi, A., Choi, T. Y., Grigoropoulos, C. P. & Komvopoulos, K. Femtosecond laser aperturless near-field nanomachining of metals assisted by scanning probe microscopy. *Appl. Phys. Lett.* **82,** 1146–1148 (2003).
5. Backus, S., Durfee III, C. G., Murnane, M. M. & Kapteyn, H. C. High power ultrafast lasers. *Rev. Sci. Instrum.* **69,** 1207–1223 (1998).
6. Keller, U. Recent developments in compact ultrafast lasers. *Nature* **424,** 831–838 (2003).
7. Brabec, T. & Krausz, F. Intense few-cycle laser fields: Frontiers of nonlinear optics. *Rev. Mod. Phys.* **72,** 545–591 (2000).
8. Steinmeyer, G., Sutter, D. H., Gallmann, L., Matuschek, N. & Keller, U. Frontiers in ultrashort pulse generation: Pushing the limits in linear and nonlinear optics. *Science* **286,** 1507–1512 (1999).
9. Boyd, R. W. *Nonlinear optics* 2nd edn (Academic, Amsterdam, 2003).
10. Kruger, J. & Kautek, W. in *Polymers and Light* Vol. 168 (ed. Lippert, T.) 247–289 (Springer, Berlin, 2004).
11. Dausinger, F., Lichtner, F. & Lubatschowski, H. *Femtosecond Technology for Technical and Medical Applications* (Springer, Berlin, 2004).
12. Bloembergen, N. A brief history of light breakdown. *J. Nonlinear Opt. Phys.* **6,** 377–385 (1997).
13. Schaffer, C. B., Brodeur, A. & Mazur, E. Laser-induced breakdown and damage in bulk transparent materials induced by tightly-focused femtosecond laser pulses. *Meas. Sci. Technol.* **12,** 1784–1794 (2001).
14. Glezer, E. N. *et al.* Three-dimensional optical storage inside transparent materials. *Opt. Lett.* **21,** 2023–2025 (1996).
15. Stuart, B. C., Feit, M. D., Rubenchik, A. M., Shore, B. W. & Perry, M. D. Laser-induced damage in dielectrics with nanosecond to subpicosecond pulses. *Phys. Rev. Lett.* **74,** 2248–2251 (1995).
16. Stuart, B. C. *et al.* Nanosecond-to-femtosecond laser-induced breakdown in dielectrics. *Phys. Rev. B* **53,** 1749–1761 (1996).
17. Bloembergen, N. Laser-induced electric breakdown in solids. *IEEE J. Sel. Top. Quant. Electron.* **10,** 375–386 (1974).
18. Schaffer, C. B., Nishimura, N., Glezer, E. N., Kim, A. M. T. & Mazur, E. Dynamics of femtosecond laser-induced breakdown in water from femtoseconds to microseconds. *Opt. Express* **10,** 196–203 (2002).
19. Sakakura, M. & Terazima, M. Initial temporal and spatial changes of the refractive index induced by focused femtosecond pulsed laser irradiation inside a glass. *Phys. Rev. B* **71,** 024113 (2005).
20. Sakakura, M., Terazima, M., Shimotsuma, Y., Miura, K. & Hirao, K. Observation of pressure wave generated by focusing a femtosecond laser pulse inside a glass. *Opt. Express* **15,** 5674–5686 (2007).
21. Sundaram, S. K. & Mazur, E. Inducing and probing non-thermal transitions in semiconductors using femtosecond laser pulses. *Nature Mater.* **1,** 217–224 (2002).
22. Chichkov, B. N., Momma, C., Nolte, S., von Alvensleben, F. & Tunnermann, A. Femtosecond, picosecond and nanosecond laser ablation of solids. *Appl. Phys. A* **63,** 109–115 (1996).
23. Liu, X., Du, D. & Mourou, G. Laser ablation and micromachining with ultrashort laser pulses. *IEEE J. Sel. Top. Quant. Electron.* **33,** 1706–1716 (1997).
24. Ashcom, J. B., Gattass, R. R., Schaffer, C. B. & Mazur, E. Numerical aperture dependence of damage and supercontinuum generation from femtosecond laser pulses in bulk fused silica. *J. Opt. Soc. Am. B* **23,** 2317–2322 (2006).
25. Tien, A. C., Backus, S., Kapteyn, H., Murnane, M. & Mourou, G. Short-pulse laser damage in transparent materials as a function of pulse duration. *Phys. Rev. Lett.* **82,** 3883–3886 (1999).
26. Streltsov, A. M. & Borrelli, N. F. Fabrication and analysis of a directional coupler written in glass by nanojoule femtosecond laser pulses. *Opt. Lett.* **26,** 42–43 (2001).
27. Will, M., Nolte, S., Chichkov, B. N. & Tunnermann, A. Optical properties of waveguides fabricated in fused silica by femtosecond laser pulses. *Appl. Opt.* **41,** 4360–4364 (2002).
28. Florea, C. & Winick, K. A. Fabrication and characterization of photonic devices directly written in glass using femtosecond laser pulses. *J. Lightwave Tech.* **21,** 246–253 (2003).
29. Osellame, R. *et al.* Optical properties of waveguides written by a 26 MHz stretched cavity Ti: sapphire femtosecond oscillator. *Opt. Express* **13,** 612–620 (2005).
30. Miura, K., Qiu, J. R., Inouye, H., Mitsuyu, T. & Hirao, K. Photowritten optical waveguides in various glasses with ultrashort pulse laser. *Appl. Phys. Lett.* **71,** 3329–3331 (1997).
31. Bruckner, R. Properties and structure of vitreous silica. I. *J. Non-Cryst. Solids* **5,** 123 (1970).
32. Glezer, E. N. & Mazur, E. Ultrafast-laser driven micro-explosions in transparent materials. *Appl. Phys. Lett.* **71,** 882–884 (1997).
33. Chan, J. W., Huser, T., Risbud, S. & Krol, D. M. Structural changes in fused silica after exposure to focused femtosecond laser pulses. *Opt. Lett.* **26,** 1726–1728 (2001).
34. Streltsov, A. M. & Borrelli, N. F. Study of femtosecond-laser-written waveguides in glasses. *J. Opt. Soc. Am. B* **19,** 2496–2504 (2002).
35. Schaffer, C. B., Garcia, J. F. & Mazur, E. Bulk heating of transparent materials using a high repetition-rate femtosecond laser. *Appl. Phys. A* **76,** 351–354 (2003).
36. Sudrie, L., Franco, M., Prade, B. & Mysyrowicz, A. Study of damage in fused silica induced by ultra-short IR laser pulses. *Opt. Commun.* **191,** 333–339 (2001).
37. Shimotsuma, Y., Kazansky, P. G., Qiu, J. R. & Hirao, K. Self-organized nanogratings in glass irradiated by ultrashort light pulses. *Phys. Rev. Lett.* **91,** 247405 (2003).

38. Bricchi, E., Klappauf, B. G. & Kazansky, P. G. Form birefringence and negative index change created by femtosecond direct writing in transparent materials. *Opt. Lett.* **29,** 119–121 (2004).
39. Kazansky, P. G. *et al.* "Quill" writing with ultrashort light pulses in transparent materials. *Appl. Phys. Lett.* **90,** 151120 (2007).
40. Rajeev, P. P. *et al.* Transient nanoplasmonics inside dielectrics. *J. Phys. B* **40,** S273–S282 (2007).
41. Brodeur, A. & Chin, S. L. Band-gap dependence of the ultrafast white-light continuum. *Phys. Rev. Lett.* **80,** 4406–4409 (1998).
42. Marburger, J. H. Self-focusing: Theory. *Prog. Quant. Electron.* **4,** 35–110 (1975).
43. Shen, Y. R. Self-focusing: Experimental. *Prog. Quant. Electron.* **4,** 1–34 (1975).
44. Alfano, R. R. & Shapiro, S. L. Observation of self-phase modulation and small-scale filaments in crystals and glasses. *Phys. Rev. Lett.* **24,** 592–594 (1970).
45. Nguyen, N. T., Saliminia, A., Liu, W., Chin, S. L. & Vallee, R. Optical breakdown versus filamentation in fused silica by use of femtosecond infrared laser pulses. *Opt. Lett.* **28,** 1591–1593 (2003).
46. Homoelle, D., Wielandy, S., Gaeta, A. L., Borrelli, N. F. & Smith, C. Infrared photosensitivity in silica glasses exposed to femtosecond laser pulses. *Opt. Lett.* **24,** 1311–1313 (1999).
47. Kamata, M. & Obara, M. Control of the refractive index change in fused silica glasses induced by a loosely focused femtosecond laser. *Appl. Phys. A* **78,** 85–88 (2004).
48. Schaffer, C. B., Brodeur, A., Garcia, J. F. & Mazur, E. Micromachining bulk glass by use of femtosecond laser pulses with nanojoule energy. *Opt. Lett.* **26,** 93–95 (2001).
49. Eaton, S. M. *et al.* Heat accumulation effects in femtosecond laser-written waveguides with variable repetition rate. *Opt. Express* **13,** 4708–4716 (2005).
50. Cheng, G. H., Wang, Y. S., Liu, Q., Zhao, W. & Chen, G. F. Study of three-dimensional storage by parallel writing in PMMA with femtosecond laser pulses. *Acta Phys. Sinica* **53,** 436–440 (2004).
51. Osellame, R. *et al.* Femtosecond writing of active optical waveguides with astigmatically shaped beams. *J. Opt. Soc. Am. B* **20,** 1559–1567 (2003).
52. Zoubir, A., Lopez, C., Richardson, M. & Richardson, K. Femtosecond laser fabrication of tubular waveguides in poly(methyl methacrylate). *Opt. Lett.* **29,** 1840–1842 (2004).
53. Sowa, S., Watanabe, W., Tamaki, T., Nishii, J. & Itoh, K. Symmetric waveguides in poly(methyl methacrylate) fabricated by femtosecond laser pulses. *Opt. Express* **14,** 291–297 (2006).
54. Davis, K. M., Miura, K., Sugimoto, N. & Hirao, K. Writing waveguides in glass with a femtosecond laser. *Opt. Lett.* **21,** 1729–1731 (1996).
55. Takeshi, F., Shimon, I., Tomoko, F., Ken, S. & Hideyuki, H. in *Photon Processing in Microelectronics and Photonics III, SPIE, San Jose, California* **5339,** 524–538 (2004).
56. Shah, L., Arai, A. Y., Eaton, S. M. & Herman, P. R. Waveguide writing in fused silica with a femtosecond fiber laser at 522 nm and 1 MHz repetition rate. *Opt. Express* **13,** 1999–2006 (2005).
57. Zhang, H., Eaton, S. M. & Herman, P. R. Low-loss Type II waveguide writing in fused silica with single picosecond laser pulses. *Opt. Express* **14,** 4826–4834 (2006).
58. Tong, L. M., Gattass, R. R., Maxwell, I., Ashcom, J. B. & Mazur, E. Optical loss measurements in femtosecond laser written waveguides in glass. *Opt. Commun.* **259,** 626–630 (2006).
59. Bhardwaj, V. R. *et al.* Femtosecond laser-induced refractive index modification in multicomponent glasses. *J. Appl. Phys.* **97,** 083102 (2005).
60. Nolte, S., Will, M., Burghoff, J. & Tuennermann, A. Femtosecond waveguide writing: A new avenue to three-dimensional integrated optics. *Appl. Phys. A* **77,** 109–111 (2003).
61. Kamata, M., Obara, M., Gattass, R. R., Cerami, L. R. & Mazur, E. Optical vibration sensor fabricated by femtosecond laser micromachining. *Appl. Phys. Lett.* **87,** 051106 (2005).
62. Sikorski, Y. *et al.* Optical waveguide amplifier in Nd-doped glass written with near-IR femtosecond laser pulses. *Electron. Lett.* **36,** 226–227 (2000).
63. Osellame, R. *et al.* Optical gain in Er-Yb doped waveguides fabricated by femtosecond laser pulses. *Electron. Lett.* **38,** 964–965 (2002).
64. Della Valle, G. *et al.* C-band waveguide amplifier produced by femtosecond laser writing. *Opt. Express* **13,** 5976–5982 (2005).
65. Taccheo, S. *et al.* Er: Yb-doped waveguide laser fabricated by femtosecond laser pulses. *Opt. Lett.* **29,** 2626–2628 (2004).
66. Gui, L., Xu, B. X. & Chong, T. C. Microstructure in lithium niobate by use of focused femtosecond laser pulses. *IEEE Photon. Tech. Lett.* **16,** 1337–1339 (2004).
67. Burghoff, J., Grebing, C., Nolte, S. & Tünnermann, A. Efficient frequency doubling in femtosecond laser-written waveguides in lithium niobate. *Appl. Phys. Lett.* **89,** 081108 (2006).
68. Shih, T., Gattass, R. R., Mendonca, C. R. & Mazur, E. Faraday rotation in femtosecond laser micromachined waveguides. *Opt. Express* **15,** 5809–5814 (2007).
69. Minoshima, K., Kowalevicz, A. M., Hartl, I., Ippen, E. P. & Fujimoto, J. G. Photonic device fabrication in glass by use of nonlinear materials processing with a femtosecond laser oscillator. *Opt. Lett.* **26,** 1516–1518 (2001).
70. Minoshima, K., Kowalevicz, A. M., Ippen, E. P. & Fujimoto, J. G. Fabrication of coupled mode photonic devices in glass by nonlinear femtosecond laser materials processing. *Opt. Express* **10,** 645–652 (2002).
71. Kowalevicz, A. M., Sharma, V., Ippen, E. P., Fujimoto, J. G. & Minoshima, K. Three-dimensional photonic devices fabricated in glass by use of a femtosecond laser oscillator. *Opt. Lett.* **30,** 1060–1062 (2005).
72. Marshall, G. D., Ams, M. & Withford, M. J. Direct laser written waveguide-Bragg gratings in bulk fused silica. *Opt. Lett.* **31,** 2690–2691 (2006).
73. Zhang, H. B., Eaton, S. M., Li, J. Z., Nejadmalayeri, A. H. & Herman, P. R. Type II high-strength Bragg grating waveguides photowritten with ultrashort laser pulses. *Opt. Express* **15,** 4182–4191 (2007).
74. Zhang, H., Eaton, S. M. & Herman, P. R. Single-step writing of Bragg grating waveguides in fused silica with an externally modulated femtosecond fiber laser. *Opt. Lett.* **32,** 2559–2561 (2007).
75. Kondo, Y. *et al.* Fabrication of long-period fiber gratings by focused irradiation of infrared femtosecond laser pulses. *Opt. Lett.* **24,** 646–648 (1999).
76. Fertein, E. *et al.* Refractive-index changes of standard telecommunication fiber through exposure to femtosecond laser pulses at 810 cm. *Appl. Opt.* **40,** 3506–3508 (2001).
77. Martinez, A., Dubov, M., Khrushchev, I. & Bennion, I. Direct writing of fibre Bragg gratings by femtosecond laser. *Electron. Lett.* **40,** 1170–1172 (2004).
78. Wikszak, E. *et al.* Erbium fiber laser based on intracore femtosecond-written fiber Bragg grating. *Opt. Lett.* **31,** 2390–2392 (2006).
79. Nikogosyan, D. N. Multi-photon high-excitation-energy approach to fibre grating inscription. *Meas. Sci. Technol.* **18,** R1–R29 (2007).
80. Sun, H. B. & Kawata, S. in *NMR - 3D Analysis - Photopolymerization* Vol. 170 (ed. Lee, S.-K.) 169–273 (Springer, Berlin, 2004).
81. Maruo, S., Nakamura, O. & Kawata, S. Three-dimensional microfabrication with two-photon-absorbed photopolymerization. *Opt. Lett.* **22,** 132–134 (1997).
82. Kawata, S., Sun, H. B., Tanaka, T. & Takada, K. Finer features for functional microdevices. *Nature* **412,** 697–698 (2001).
83. LaFratta, C. N., Fourkas, J. T., Baldacchini, T. & Farrer, R. A. Multiphoton Fabrication. *Angew. Chem. Int. Edn* **46,** 6238–6258 (2007).
84. Sun, H. B., Matsuo, S. & Misawa, H. Three-dimensional photonic crystal structures achieved with two-photon-absorption photopolymerization of resin. *Appl. Phys. Lett.* **74,** 786–788 (1999).
85. Deubel, M. *et al.* Direct laser writing of three-dimensional photonic-crystal templates for telecommunications. *Nature Mater.* **3,** 444–447 (2004).
86. Berns, M. W., Olson, R. S. & Rounds, D. E. *In vitro* production of chromosomal lesions with an argon laser microbeam. *Nature* **221,** 74–75 (1969).
87. Liang, H., Wright, W. H., Cheng, S., He, W. & Berns, M. W. Micromanipulation of chromosomes in Ptk2 cells using laser microsurgery (optical scalpel) in combination with laser-induced optical force (optical tweezers). *Exp. Cell Res.* **204,** 110–120 (1993).
88. Berns, M. W. *et al.* Laser micro-surgery in cell and developmental biology. *Science* **213,** 505–513 (1981).
89. Vogel, A., Noack, J., Huttman, G. & Paltauf, G. Mechanisms of femtosecond laser nanosurgery of cells and tissues. *Appl. Phys. B* **81,** 1015–1047 (2005).
90. König, K., Riemann, I., Fischer, P. & Halbhuber, K. H. Intracellular nanosurgery with near infrared femtosecond laser pulses. *Cell. Mol. Biol.* **45,** 195–201 (1999).
91. Watanabe, W. *et al.* Femtosecond laser disruption of subcellular organelles in a living cell. *Opt. Express* **12,** 4203–4213 (2004).
92. Shen, N. *et al.* Ablation of cytoskeletal filaments and mitochondria in live cells using a femtosecond laser nanoscissor. *Mech. Chem. Biosystems* **2,** 17–25 (2005).
93. Supatto, W. *et al. In vivo* modulation of morphogenetic movements in *Drosophila* embryos with femtosecond laser pulses. *Proc. Natl Acad. Sci. USA* **102,** 1047–1052 (2005).
94. Yanik, M. F. *et al.* Functional regeneration after laser axotomy. *Nature* **432,** 822 (2004).
95. Chung, S. H., Clark, D. A., Gabel, C. V., Mazur, E. & Samuel, A. D. T. The role of the AFD neuron in C-elegans thermotaxis analyzed using femtosecond laser ablation. *Bmc Neuroscience* **7,** 30 (2006).
96. Watanabe, W., Onda, S., Tamaki, T., Itoh, K. & Nishii, J. Space-selective laser joining of dissimilar transparent materials using femtosecond laser pulses. *Appl. Phys. Lett.* **89,** 021106 (2006).
97. Tamaki, T., Watanabe, W., Nishii, J. & Itoh, K. Welding of transparent materials using femtosecond laser pulses. *Jpn J. Appl. Phys.* **44,** L687–L689 (2005).
98. Watanabe, W., Onda, S., Tamaki, T. & Itoh, K. Direct joining of glass substrates by 1 kHz femtosecond laser pulses. *Appl. Phys. B* **87,** 85–89 (2007).
99. Tamaki, T., Watanabe, W. & Itoh, K. Laser micro-welding of transparent materials by a localized heat accumulation effect using a femtosecond fiber laser at 1558 nm. *Opt. Express* **14,** 10460–10468 (2006).
100. Miura, K., Qiu, J. R., Mitsuyu, T. & Hirao, K. Space-selective growth of frequency-conversion crystals in glasses with ultrashort infrared laser pulses. *Opt. Lett.* **25,** 408–410 (2000).
101. Yu, B. *et al.* Study of crystal formation in borate, niobate, and titanate glasses irradiated by femtosecond laser pulses. *J. Opt. Soc. Am. B* **21,** 83–87 (2004).
102. Miura, K., Qiu, J. R., Fujiwara, S., Sakaguchi, S. & Hirao, K. Three-dimensional optical memory with rewriteable and ultrahigh density using the valence-state change of samarium ions. *Appl. Phys. Lett.* **80,** 2263–2265 (2002).
103. Manz, A., Graber, N. & Widmer, H. M. Miniaturized total chemical-analysis systems - A novel concept for chemical sensing. *Sens. Actuators B* **1,** 244–248 (1990).
104. Reyes, D. R., Iossifidis, D., Auroux, P. A. & Manz, A. Micro total analysis systems. 1. Introduction, theory, and technology. *Anal. Chem.* **74,** 2623–2636 (2002).
105. Auroux, P. A., Iossifidis, D., Reyes, D. R. & Manz, A. Micro total analysis systems. 2. Analytical standard operations and applications. *Anal. Chem.* **74,** 2637–2652 (2002).
106. Marcinkevicius, A. *et al.* Femtosecond laser-assisted three-dimensional microfabrication in silica. *Opt. Lett.* **26,** 277–279 (2001).
107. Kondo, Y., Qiu, J., Mitsuyu, T., Hirao, K. & Yoko, T. Three-dimensional microdrilling of glass by multiphoton process and chemical etching. *Jpn J. Appl. Phys.* **38,** L1146–L1148 (1999).
108. Masuda, M. *et al.* 3-D microstructuring inside photosensitive glass by femtosecond laser excitation. *Appl. Phys. A* **76,** 857–860 (2003).
109. Maselli, V. *et al.* Fabrication of long microchannels with circular cross section using astigmatically shaped femtosecond laser pulses and chemical etching. *Appl. Phys. Lett.* **88,** 191107 (2006).
110. Chiodo, N. *et al.* Imaging of Bloch oscillations in erbium-doped curved waveguide arrays. *Opt. Lett.* **31,** 1651–1653 (2006).
111. Szameit, A. *et al.* Two-dimensional soliton in cubic fs laser written waveguide arrays in fused silica. *Opt. Express* **14,** 6055–6062 (2006).
112. Pierce, J. R. Coupling of modes of propagation. *J. Appl. Phys.* **25,** 179–183 (1954).
113. Bellouard, Y., Said, A., Dugan, M. & Bado, P. Fabrication of high-aspect ratio, micro-fluidic channels and tunnels using femtosecond laser pulses and chemical etching. *Opt. Express* **12,** 2120–2129 (2004).


## Acknowledgments

The authors would like to acknowledge C. R. Mendonca, J. Dowd, M. Haider-Syed and T. Baldacchini for input on the manuscript. The authors are supported by the Army Research Office under contract W911NF-05-1-0471.